

Supplementary material

Title: Synergistic Effects of Iron Oxide Nanoparticles and Hydrogen Peroxide in Inhibiting *Pseudomonas aeruginosa* Growth to Combat Bacterial Contamination in Water Recovery Systems

Omid Sedighi¹, Tucker Johnsen¹, Appala Raju Badireddy², Matthew J. Wargo³, Amber L. Doiron^{1*}

- **XRD results:**

According to Scherrer's equation, $t = \lambda / \beta \cos \theta$, average particles size (t) can be estimated by XRD pattern. In the Scherrer's equation λ , β , and θ stand for the wavelength of Cu K α radiation, width of the peak at half of the maximum, and Bragg angle, respectively. The average β of the peaks related to the PAA@IONPs were wider (20 ± 12) than uncoated IONPs, suggesting that the particle size of coated samples should be smaller than uncoated ones.

- **FTIR results:**

PAA coated samples could not be lyophilized due to the hydrophilic and viscoelastic properties of PAA, which promotes water retention and forms a viscoelastic gel matrix during sublimation, impeding efficient water removal and resulting in a fibrous structure rather than a compact powder. Thus, PAA@IONPs were dried in the oven at 70 °C overnight. Since the oven was not under vacuum, oxidation could have occurred during the drying process. To account for this, bare IONPs were dried separately in a lyophilizer (Freezone 2.5, Labconco, USA) and oven to compare the data. For both drying techniques, prominent absorption bands were observed at approximately 610 cm⁻¹, which was associated with the Fe-O bond vibration. A broad stretching band was observed between 3200-3500 cm⁻¹, which suggested the presence of -O-H groups from water molecules that were adsorbed and hydrogen bonded to the surface of the IONPs. The higher intensity of these bands in the sample dried in the oven suggested an increased presence of these adsorbed water molecules, reflecting enhanced surface adsorption due to the drying process. Pure polyacrylic acid samples showed all the peaks related to surface functional groups of PAA, including a strong peak at 1718 cm⁻¹ that is associated with -C=O band, corresponding to carboxylate group on the surface of PAA. However, in PAA@IONPs, the intensity of this peak decreased substantially and the peak of COO⁻ stretching band at 1410 cm⁻¹ was present. The distinct bands in the spectra of both IONPs and PAA indicate the high purity of these chemicals.

- **XPS results:**

Similar to previous observations from FTIR, PAA@IONPs could not be effectively dried using a freeze-dryer; thus, oven drying was necessary. Post-oven drying, a noticeable color change from black to a slightly oxidized brown color was observed, suggesting potential oxidation. To ascertain whether oxidation occurred during synthesis or drying, IONPs were dried using both a freeze-dryer and an oven. The XPS results, displayed in Figure 3, indicated the presence of characteristic Fe 2p_{3/2} and Fe 2p_{1/2} peaks at 711.1 eV and 724.3 eV, respectively, across all samples. According to the literature, the characteristic binding energies for Fe 2p_{3/2} and Fe 2p_{1/2} are 710.35 eV and 724.0 eV for γ -Fe₂O₃, and 711.29 eV and 724.82 eV for Fe₃O₄, respectively [32]. This confirms that our samples predominantly consist of Fe₃O₄. Notably, a satellite peak at 718.5 eV was detected exclusively in samples dried in the oven. This satellite peak is typically associated with the presence of γ -Fe₂O₃ [33-35]. The absence of this peak in the sample dried using a freeze-dryer, implied that the freeze-drying process preserved the oxidation state of the magnetic nanoparticles without further oxidation. In contrast, the oven-dried samples likely underwent oxidation due to the high temperature (70 °C) exposure in an oxygen-rich environment.

While uncoated samples showed no C 1s peak, the PAA@IONPs sample exhibited this peak (as shown in Figure 1a), indicating the presence of carbon from the PAA coating. Moreover, the low intensity of the C=O peaks compared to the high-intensity peak of C-O, further confirms that the bonding between the iron ions in the core and the PAA occurred through the breakage of C=O bonds within the PAA structure, which is in agreement with FTIR data. Lastly, the O 1s peak for the uncoated samples displayed typical iron oxide bindings, whereas the coated samples exhibited varied oxygen bindings, suggesting additional chemical interactions facilitated by the PAA coating (Figure 1b,c).

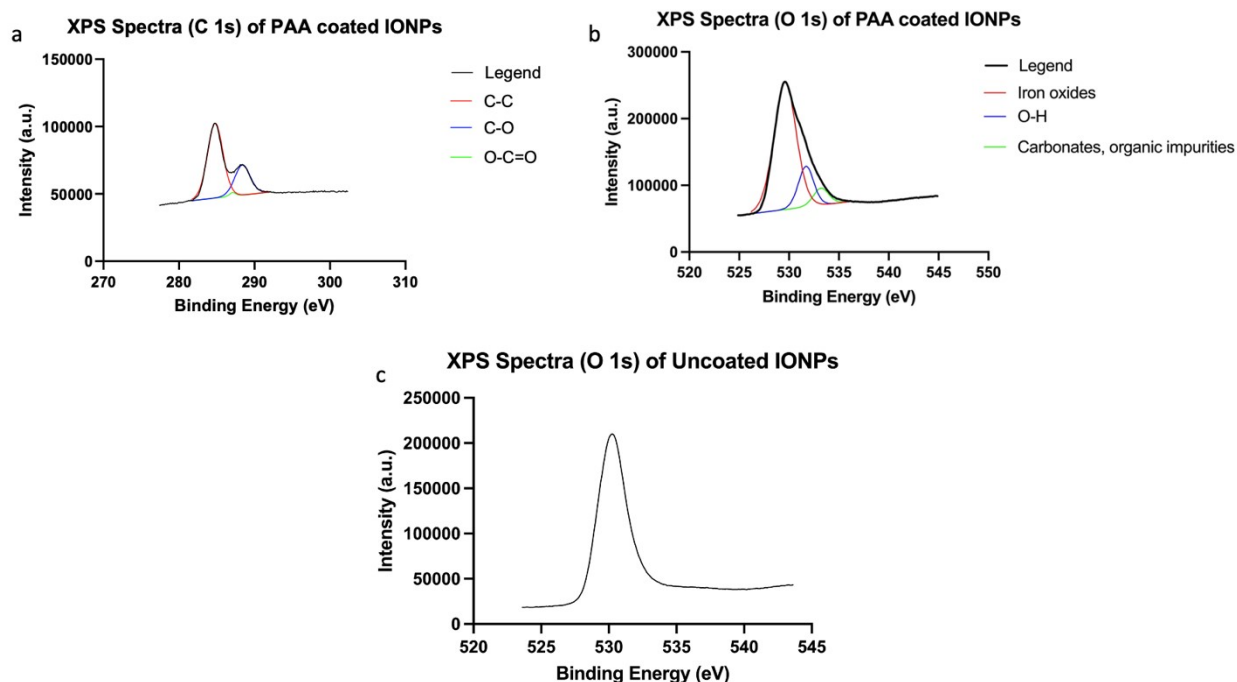


Figure 1 XPS analysis, (a) C 1s XPS spectra of PAA@IONPs, O 1s XPS spectra of (b) PAA@IONPs, and (c) IONPs.

• Coating enhanced colloidal stability of IONPs

Images of storage analysis, shown in Figure 2a-d, provide qualitative insight into the colloidal stability of the coated and bare nanoparticles. If the solution color remained unchanged after a week of storage, the particles remained uniformly suspended in the aqueous medium. In contrast, lighter-colored solutions at the top exhibited more particle precipitated at the bottom of the vials, as indicated by the arrows. Our results showed that PAA@IONPs displayed less precipitation, higher colloidal stability than uncoated IONPs.

UV-vis analysis was used to quantify the number of suspended particles, which is suggestive of the colloidal stability of synthesized nanoparticles. At various intervals and without disturbing particles at the bottom of the vial, the absorbance of remaining suspended particles was measured at 350 nm, as shown in Figure 2e. A lesser change in absorbance suggests higher colloidal stability. The data reveal that after a week of storage, the peak intensity of bare IONPs decreased by 60%, while PAA@IONPs showed a 22% decrease, demonstrating that the coating can substantially enhance the colloidal stability of IONPs over time.

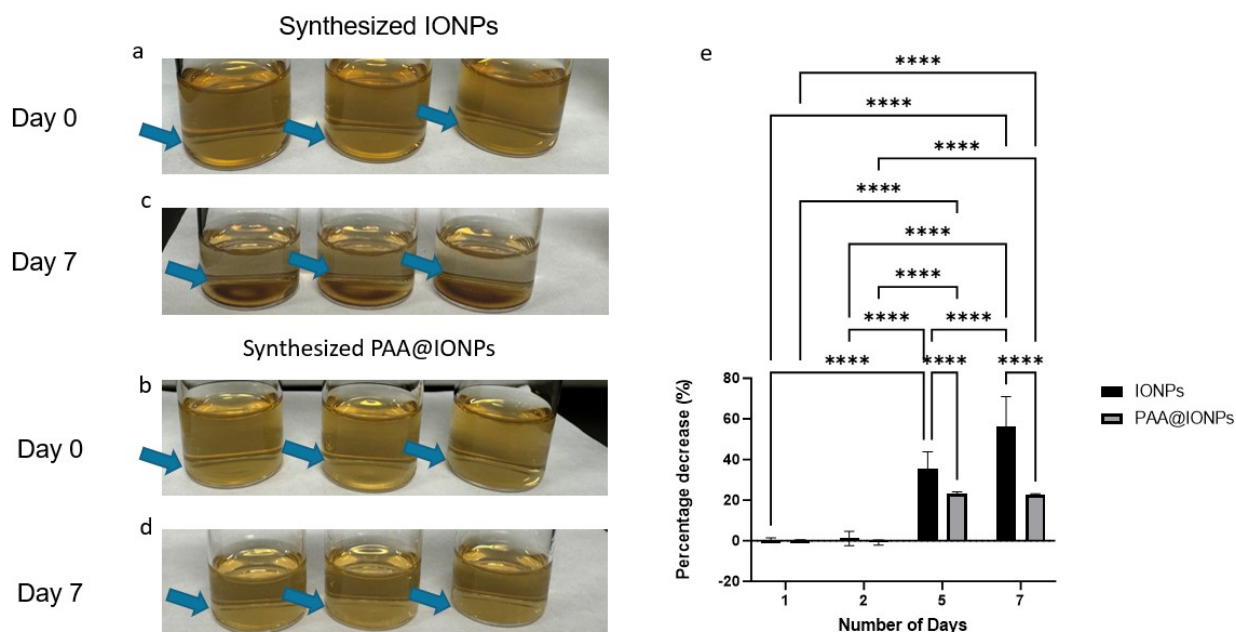


Figure 2 Sedimentation behavior of synthesized IONPs, and PAA@IONPs. (a,c), and (b,d) Images presented are a side-view of 20 ml scintillation vials at day 0 immediately after being sonicated and seven days later from the same view but without any mixing for IONPs and PAA@IONPs, respectively. Arrows indicate precipitation at the bottom of the vial after a week. (e) Stability testing of IONPs using UV-vis to evaluate the percentage change in absorbance over time in water. $n = 3$, **** $p < 0.0001$.

• Zeta potential lower for PAA@IONPs than IONPs

As another means of assessing colloidal stability, zeta potential measurements were conducted on IONPs and PAA@IONPs to assess their electrochemical and surface charge characteristics, as shown in Figure 3. Values further from zero generally suggest better colloidal stability due to increased electrostatic repulsion between particles. The PAA coating increased the zeta potential values in a statistically significant manner.

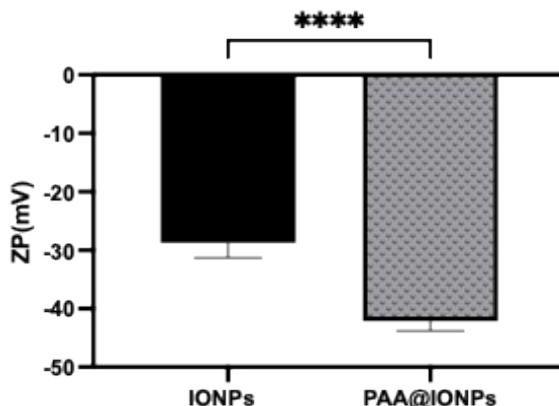


Figure 3 Zeta potential of synthesized IONPs and PAA@IONPs. $n=3$, **** $p < 0.0001$.

- **Effect of hydrogen peroxide on bacterial growth is concentration-dependent**

Figure 4 illustrates the effects of various concentrations of hydrogen peroxide on bacterial growth. Figure 4a shows that concentrations 16 mM and below did not significantly impact bacterial growth. Conversely, Figure 4b reveals that 2000 and 400 mM hydrogen peroxide completely halted bacterial growth. To find a concentration that impacts growth but does not completely eradicate the bacteria, another series of tests with smaller intervals was conducted. Figure 4c indicates that concentrations above 81 mM significantly reduced bacterial growth, and at 182.25 mM, growth dropped to approximately 50%. Consequently, 182.25 mM was selected as the concentration for further studies on the impact of IONPs on bacterial growth inhibition through the generation of radical ROS (Eq 1 and 2 in the main manuscript).

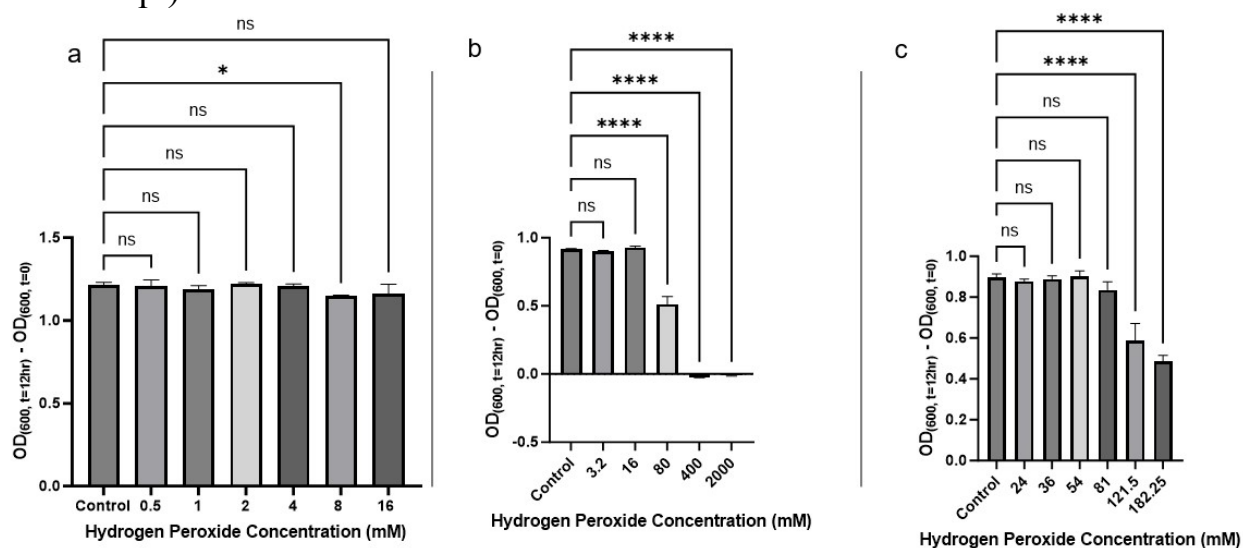


Figure 4 Impact of various hydrogen peroxide concentrations on bacterial growth over 12 hr of incubation, n=3 **** $p < 0.0001$, * $p = 0.0447$. ns= not significant

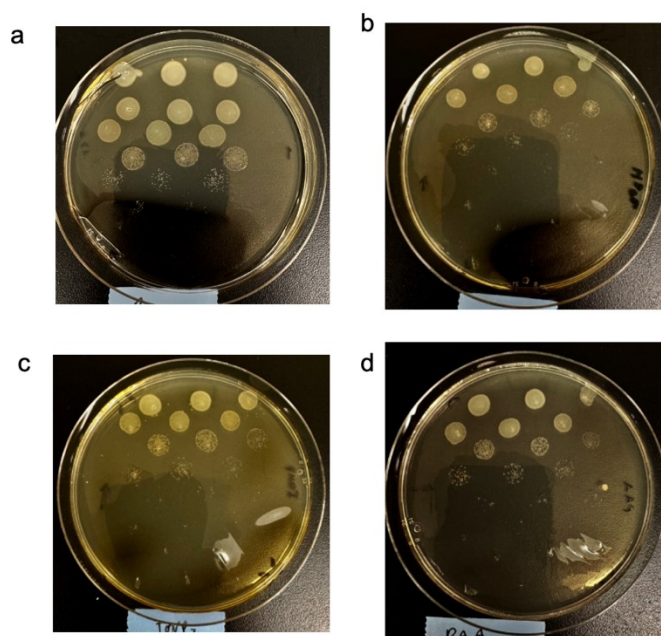


Figure 5 Spot dilution antibacterial study of (a) bacteria sample, (b) H_2O_2 + Bacteria, (c) IONPs+ H_2O_2 +bacteria, and (d) PAA@IONPs+ H_2O_2 +bacteria.